

WEAK LINEAL VARIATION OF THE NEUMANN BOUNDARY CONDITIONS IN A SUPERCONDUCTING PLATE

José José Barba-Ortega, Carlos Andrés Sjogreen Blanco, Miryam R-Joya

Abstract: Few theoretical studies of the thermodynamics properties in superconductors have been carried out in situations where the sample is in contact with an anisotropic material. Thus, the physical properties of the material in contact with the superconductor could vary in the sample surface. In this contribution are studying the superconducting properties of a Niobium prism with its lateral surfaces in contact with deferent kinds of metallic and/or superconducting materials. Numerically has been modelling an engineering boundary condition or anisotropic frontier via the deGennes penetration length b . The inverse of b vary linearly on the surfaces of the sample as $\gamma=1-\delta/b$ (δ is the size of the mesh grid). The second thermodynamic field increase when $b<0$ is considered and a slowly entry of the magnetic field is observed in the metallic regions of the boundary.

Keywords: deGennes parameter, Inhomogeneous surface, Superconductor.

VARIACIÓN LINEAL DÉBIL DE LA CONDICIÓN DE FRONTERA DE NEUMANN EN UNA PLACA SUPERCONDUCTORA

Resumen: Pocos estudios teóricos sobre propiedades termodinámicas en los superconductores se han llevado a cabo en situaciones en que la muestra está en contacto con un material aniso-trópico. Por lo tanto, las propiedades físicas del material en contacto con el superconductor podrían variar en la superficie de la muestra. En esta contribución, se estudian las propiedades superconductoras de un prisma de niobio con sus superficies laterales en contacto con diferentes tipos de metales y/o materiales superconductores. Numéricamente se ha modelado una condición de contorno de ingeniería o frontera aniso-trópico a través de la longitud de penetración deGennes b . El inverso de b varía linealmente sobre las superficies de la muestra como $\gamma=1-\delta/b$ (δ es el tamaño de la rejilla en la malla). El segundo campo termodinámico aumenta cuando se considera $b<0$ y una entrada lentamente del campo magnético se observa en las regiones metálicas de la frontera.

Palabras clave: Parámetro deGennes, Superficie no homogénea, Superconductor.

Recibido (21/07/15), aceptado (05/11/15). los Dres. José José Barba-Ortega y Miryam R-Joya, y el MSc. Carlos Andrés Sjogreen Blanco desempeñan sus actividades en la Universidad Nacional de Colombia, Bogotá D.C., Colombia. Correos electrónicos: jjbarbao@unal.edu.co, mrinconj@unal.edu.co y casjogreenbl@unal.edu.co

1. INTRODUCTION

The study of the superconducting state at mesoscopic level is an important topic of investigation due to its technological potential applications, applications such as SQUID manufacturing [1], microwave circuits [2-4] among others. It is well known that the main difference of the magnetic behaviour of such materials between mesoscopic and macroscopic levels is that the geometry and size of the sample dramatically influence its magnetic response. In this type of sample, the competition among the surface currents, the external applied magnetic field and the defects of the crystal lattice become relevant, leading to fascinating new vortex structures. Multiple theoretical studies have been carried out with several geometries, such as cones [5], spheres [6], discs [7], prisms, solid of revolution [8]. At experimental level, the interplay charge/vortices in a superconducting coulomb-blockaded island was studied [9], D. Roditchev et al., observed Josephson vortex cores in a superconducting-insulating-superconducting heterostructure (S-I-S), he show a vortex Josephson generation by applying supercurrents through electrical means without magnetic field, which is a crucial step towards high-density on-chip integration of superconducting quantum devices [10], I. Lukyanchuk, et al. studied the Rayleigh instability of vortex droplets in superconductors, he found the dynamics of Abrikosov-Nielsen-Olesen vortices in systems with effects in quantum field theory by means of bench-top laboratory experiments [11]. In this paper, are analysed the effects of an anisotropic boundary condition on the vortex configurations and critical fields. In fact, this system has an experimental ground because it is based on the fact that substrates on which are deposited the superconducting samples are generally inhomogeneous, presenting different properties at the contact edge of the sample, which could affect their magnetic behaviour. In the following sections are showing some theoretical concepts necessary to put in context the reader, and finally presented some results and discuss them.

THEORETICAL FORMALISM

According to the Ginzburg-Landau formalism [12, 13, 14] the order parameter Ψ and de vector potential \vec{A} can be associated through equations 1 and 2. These equations are scaled as follows Ψ in units of $(\alpha\beta)^{1/2}$, where α and β are two proper phenomenological parameters of the material, the distances are in units of coherence length $\xi(0)$, time is in units of $\pi\hbar/(96K_B T_c)$, the vector potential A in units of $H_{c2}\xi$ and Gibbs free energy, G in units of $(\alpha T_c)^2/\beta$.

$$\frac{\partial\Psi}{\partial t} = -\frac{1}{\eta}\left((-i\nabla - \vec{A})^2\Psi + (|\Psi|^2 - 1)\Psi\right) \quad (1)$$

$$\frac{\partial\vec{A}}{\partial t} = Re[\Psi^*(-i\nabla - \vec{A})\Psi] - \kappa^2\nabla \times \nabla \times \vec{A} \quad (2)$$

Boundary condition complement equations 1 and 2, where $b=\delta/(1-\gamma)$ is the deGennes parameter, δ is the mesh size and \hat{n} is the unit normal vector to the surface [15].

$$\hat{n} \cdot \left(-i\hbar\nabla + \frac{e^*}{c}\vec{A}\right)\Psi\Big|_n = -\frac{i\hbar}{\delta}(1-\gamma)\Psi\Big|_n \quad (3)$$

$$\gamma(x) = \gamma_1 + (x/L)(\gamma_2 - \gamma_1) \quad (4)$$

From equation 4, have $\gamma(x=0)=\gamma_1$ e $\gamma(x=L)=\gamma_2$ and $\gamma_2>\gamma_1$. $b\rightarrow\infty$, ($\gamma=1$) simulates vacuum/insulator superconducting boundary, $\delta>b>0$ ($0<\gamma<1$) identifies a superconductor-metal boundary, leading to a superconductivity is suppressed at the material edge. $b<0$, ($\gamma>1$) simulates a superconducting interface in contact with another superconductor at higher critical temperature. The method of linking variables was used for the discretization and solution of the Ginzburg-Landau equations (method ΨU) [16, 17]. All this condition imply that super-currents cannot flow out of the superconductor ($J_s=0$).

RESULTS AND DISCUSSION

The Ginzburg-Landau equations for a square sample of lateral dimensions $L=L_x=L_y=12\xi(0)$, were numerically solved taking the mesh size $\delta = a_x = a_y = 0.1$. The order parameter and the vector potential were taken invariants on the z axis in which the external magnetic field H is applied, therefore, the demagnetization effects can be neglected in z axes [20]. The Ginzburg-Landau parameter $\kappa = \lambda/\xi$ is a typical value for N_b , $T = 0$ in all cases. For better analysis is used $\gamma = 1 - a_x/b$, which varies linearly through the boundaries parallels to the x axis. In this paper are taken two gradients, for gradient 1 (∇_1), considering a purely superconductor-metal boundary, where the sample metallic character in contact with the superconductor varies as $\gamma = 0.75$ at $x = 0$ to $\gamma = 0.80$ at $x = L_x$, so b is in the range $0.4 \leq b \leq 0.5$, and similarly by considering the gradient 2 (∇_2), taking into account that at some point of the sample material in contact with the superconductor is no longer a metal and becomes a superconductor at higher critical temperature, in other words $b<0\rightarrow b=0\rightarrow b>0$. In this case $\gamma = 0.1$ at $x = 0$ to $\gamma = 1.1$ at $x = L_x$, b is in the range $-1.1 \leq b \leq 9.0$, which means that the boundary section at $x=0$ is in contact with a metal, while $x=L_x$ is in contact with a higher T_c superconductor. On the other hand, lateral boundaries parallel to the y axis are in contact with vacuum, $b\rightarrow\infty$.

Figure 1 shows the curves of the Gibbs free energy G for ∇_1 and ∇_2 selected as a function of the applied magnetic field. Throughout of all magnetic field loop is satisfied the condition $G(\nabla_2) \ll G(\nabla_1)$. This result clearly identifies that the Beam-Livingston surface energy decreases by considering a superconductor/metal surface [18, 19]. Transition fields H_p between different vortices states are different for $H < 0.4$, and very similar for $H > 0.4$ when the magnetic field decreases. Considering the two gradients, the magnetic field for the first vortex chain entry H_{p1} occurs in $H_{p1} = 0.71$.

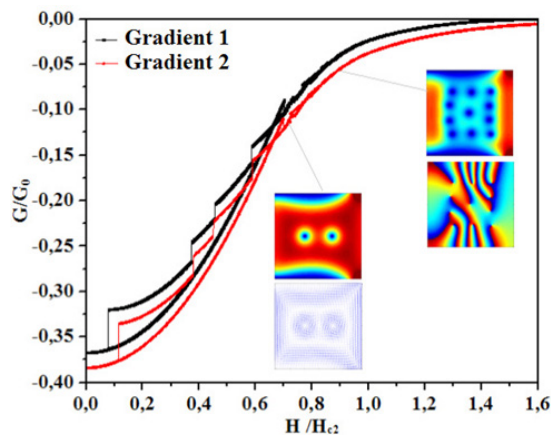


Figure 1. Gibbs free energy for ∇_1 and ∇_2 as a function of the magnetic field.

The magnetization curves for the two gradients of γ are showed in Figure 2. It is observed that the two curves overlap to $H \approx 1.0$, from this value the $-4\pi M$ is grater for ∇_2 than for ∇_1 , which means that for $H > 1.0$ the energy barrier effect becomes noticeable and the diamagnetism of the sample decrease. Due to $dG \sim -MdB$, the difference in magnetization for the two gradients explains the discrepancy between G values found in Figure 1.

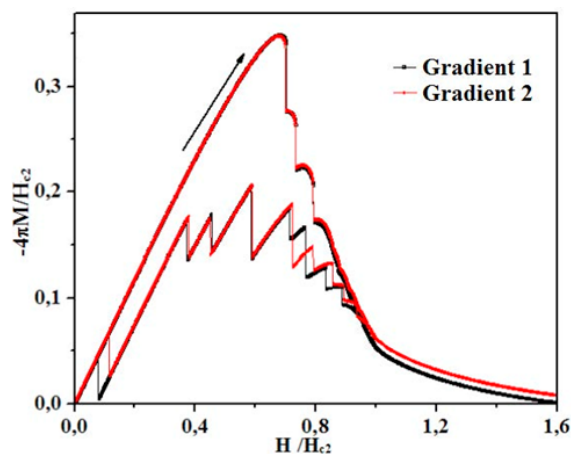


Figure 2. Magnetization curves for ∇_1 and ∇_1 for a loop of the magnetic field.

The vortex number and the order parameter as a function of the applied magnetic field for the two gradients is shown in Figure 3. It can be seen that $(H_{p1}(\nabla_2) > H_{p1}(\nabla_1))$ around the field loop. Increasing the magnetic field, the vortex transition occurs at $1 \rightarrow 3 \rightarrow 5 \rightarrow 7$ to $H = 0.9$ where transition $L \rightarrow L+1$ takes place. By decreasing H , sample vortices output occurs irregularly. At $H = 0$ no vortex is trapped, inferring that the irregular surface does not act as a vortices anchor. Additionally, in the same figure is also shown $|\Psi|^2$ for three different magnetic fields as evidenced that the vortices entry the sample through irregular boundary.

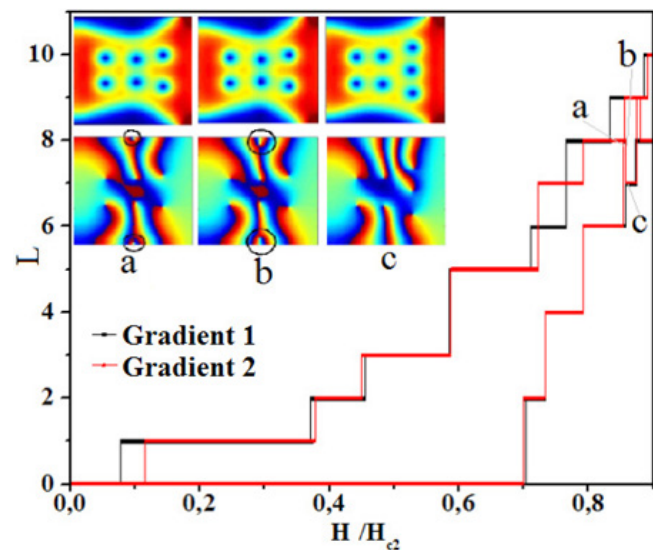


Figure 3. Vorticity and square modulus of the order parameter for ∇_1 and ∇_2 case as a function of the magnetic field.

Figure 4 shows the Cooper pairs density ($|\Psi|^2$), its phase and the supercurrents for 5 different values of H . It can be observed that for ∇_1 the area near the boundary parallel to the x axis where for low fields the superconductivity is suppressed because of metal presence. For $H \approx 1.0$, a higher reduction of order parameter is shown in the middle area, in this case the small difference between the chosen values of γ does not affect conventional and well-known symmetry of the magnetic field entry.

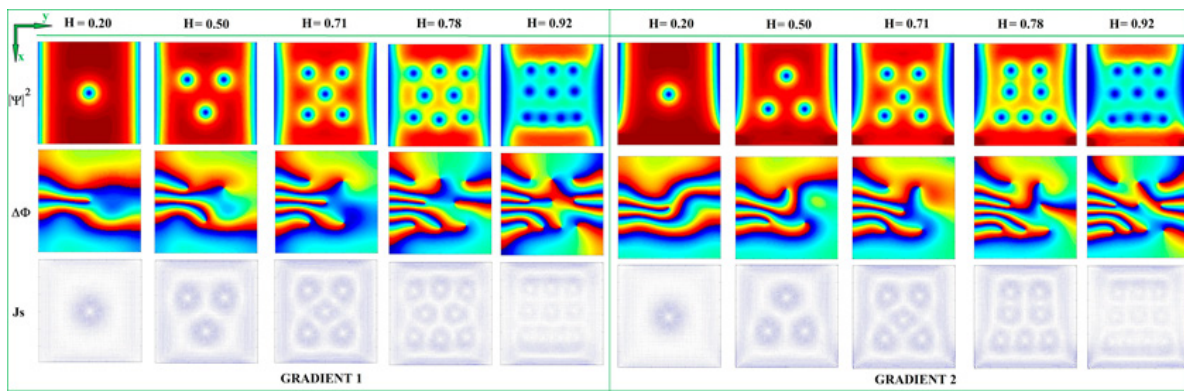


Figure 4. Super-electrons density $|\Psi|^2$, phase $\Delta\Phi$, and super-current J_s of both gradients for different magnetic fields values.

There is a clear difference between the region in which occurs the vortex penetration for ∇_2 and ∇_1 . In ∇_2 this region is not uniform across the boundary and gradually fades over it, while ∇_1 is uniform. The superconducting/superconducting at higher critical temperature T_c makes $|\Psi|^2$ increases.

There is another difference between the two developed gradients, this occurs at $H = 0.5$, although in both cases there are three vortices, its topological configuration is different. This is explained because each configuration enables an energetically more favourable state for each gradient, and it is related to the presence of the Bean-Livingston energy barrier, since the vortices tend to enter areas where $b > 0$ (superconductivity reduction), the boundary condition superconducting-higher T_c superconductor allows vortices inputs at higher magnetic fields than in a superconducting-metal boundary. It can be seen different vortex configurations in the studied cases.

CONCLUSIONS

In the presence of an applied magnetic field the time-dependent Ginzburg Landau equations for a square sample are numerically solved. Two parallel faces of the square are in vacuum contact while the other two are in inhomogeneous material contact. Two cases have been analysed, one with a variable metallic contact surface and another presenting a smoothly variation of a metal-ferromagnetic ($b=0$)-superconducting contact surface. Both cases studied show that $H_{p1}(\nabla_2) > H_{p1}(\nabla_1)$, therefore the Bean Livingstone is higher for ∇_1 , because this surface energy barrier is responsible for H values in which the vortices entry/exit the mesoscopic sample.

ACKNOWLEDGEMENTS

The author would like to thank professor Edson Sardella of the Department of Physics of the Estadual Paulista University, Bauru, Brazil, for his very useful discussions.

REFERENCES

- [1] H. J. Brake, "SCENET roadmap for superconductor digital electronics", *Physica C*, vol. 439, 2006, p. 1.
- [2] V. Sokolovsky, L. Prigozhin, V. Dikovskiy, "Meissner transport current in flat films of arbitrary shape and a magnetic trap for cold atoms", *Sci. Technol.*, vol. 23, 2010, p. 065003.
- [3] J. Pearl, "Current distribution in superconducting films carrying quantized fluxoid", *Appl. Phys. Lett.*, vol 5, no 4, 1964, p. 65.
- [4] E. Bustarret, "Superconductivity in doped semiconductors", *Physica C*, vol. 514, 2015, p. 36.
- [5] Y. Chen, M. M. Doria, F. M. Peeters, "Vortices in a mesoscopic cone: A superconducting tip in the presence of an applied field", *Phys. Rev. B*, vol. 77, 2008, p. 054511.
- [6] B. Xu, M. V. Milosevic, F. M. Peeters, "Magnetic properties of vortex states in spherical superconductors", *Phys. Rev. B*, vol. 77, 2008, p. 144509.
- [7] M. M. Doria, R. M. Romaguera, F. M. Peeters, "Effect of the boundary condition on the vortex patterns in mesoscopic three-dimensional superconductors: Disk and sphere", *Phys. Rev. B*, vol. 75, 2007, p. 064505.

- [8] A. Shitade and Y. Nagai, "Orbital angular momentum in a nonchiral topological superconductor", *Phys. Rev. B*, vol. 92, 2015, p. 024502.
- [9] I. M. Khaymovich, V. F. Maisi, J. P. Pekola, and A. S. Melnikov, "Charge-vortex interplay in a superconducting Coulomb-blockaded island", *Phys. Rev. B*, vol 92, 2015, p 020501.
- [10] D. Roditchev, C. Brun, L. Serrier, J. C. Cuevas, V. H. Loiola, M. V. Milosevic, F. Debontridder, V. Stolyarov and T. Cren, "Direct observation of Josephson vortex cores", *Nature Physics*, vol.11, 2015, p. 332.
- [11] I. Lukyanchuk, V. M. Vinokur, A. Rydh, R. Xie, M. V. Milosevic, U. Welp, M. Zach, Z. L. Xiao, G. W. Crabtree, S. J. Bending, F. M. Peeters and W. K. Kwok, "Rayleigh instability of confined vortex droplets in critical superconductors", *Nature Physics*, vol. 11, 2015, p. 21.
- [12] J. Barba-Ortega, E. Sardella, J. A. Aguiar, "Superconducting properties of a parallelepiped mesoscopic superconductor: A comparative study between the 2D and 3D Ginzburg-Landau models", *Phys. Lett. A.*, vol. 379, no. 7, 2015, p. 732.
- [13] J. Barba-Ortega, E. Sardella, J. A. Aguiar, "Superconducting boundary conditions for mesoscopic circular samples", *Supercond. Sci. Technol.*, vol. 24, 2011, p. 015001.
- [14] M.V. Milosevic, "The Ginzburg-Landau theory in application", *Physica C*, vol. 470, 2010, p. 791.
- [15] P. G. de Gennes, "Superconductivity of Metals and Alloys", New York: Addison-Wesley, 1994, p. 274.
- [16] A. C. Bolech, G. C. Buscaglia, A. Lopez, "Connectivity and Superconductivity", ed. J. Berger, J. Rubinstein, Berlin: Springer-Verlag, 2000.
- [17] D. Gropp, H. G. Kaper, G. K. Leaf, D. M. Levine, M. Palumbo, V. M. Vinokur, "Numerical simulation of vortex dynamics in type-II superconductors", *J. Comput. Phys.*, vol. 123, 1996, p. 254.
- [18] C. P. Bean and J. D. Livingston, "Surface Barrier in Type-II Superconductors", *Phys. Rev. Lett.*, vol 12, 1964, p. 14.
- [19] C. C. de Souza Silva, J. A. Aguiar, "Irreversible matching effects in homogeneous and layered superconducting films", *Physica C*, vol. 354, 2001, p. 232.
- [20] F. Rogeri, R. Zadorosny, P. N. Lisboa-Filho, E. Sardella and W. A. Ortiz, "Magnetic field profile of a mesoscopic SQUID-shaped superconducting film", *Supercond. Sci. Technol.*, vol 26, 2013, p. 075005.